

# Mechanism Design for Variable Stiffness Actuation based on Enumeration and Analysis of Performance

Manuel G. Catalano, Riccardo Schiavi, and Antonio Bicchi

**Abstract**—This paper presents a systematic enumeration and performance analysis of Variable Stiffness Actuators (VSAs). VSAs are becoming more and more popular in robotics, and many different prototypes have been recently proposed and built in the research community. In comparison with conventional geared motors, actuators with variable stiffness introduce the need for new specifications, requirements, and performance criteria, concerning e.g. the range of achievable stiffness, and the response time to stiffness reference changes. On the other hand, the mechanical construction of VSAs is also more complex. To address the problem of harnessing the increased complexity of VSA design, we consider in this article the enumeration of all possible arrangements of two prime movers (elementary motors), two harmonic-drive gears, the output shaft, and the interconnections (either rigid or elastic) between these elements. We propose an automated algorithm to search the large combinatorics of such enumeration, and present a reduced number of feasible basic designs which accomplish the objectives of VS actuation. Furthermore, we propose a quasi-static model of VS actuators which can be used for an analysis of their performance and we conclude by presenting some preliminary characteristics of one of the selected designs.

**Index Terms**—Physical Human-Robot Interaction, Safety, Performance, Variable Stiffness Mechanisms, Actuators

## I. INTRODUCTION

Applications requiring physical Human-Robot Interaction (pHRI) occur more and more frequently in both advanced industrial automation and service robotics. Such applications require ever more stringent requirements on safety and dependability, adaptability, and ultimately on the capability of exhibiting a human-friendly behaviour. To address such issues, several researchers in the past few years have proposed novel actuators which can vary their stiffness in accordance to the task needs (Variable Stiffness Actuators (VSA), [1], [2]). Moreover, VSAs allow to adapt to the task the system resonant frequency ([3], [4]), thus reducing energy consumption during repetitive task and achieving more natural motions ([5]) adapting the joint stiffness to the task and the environment.

The VSA idea is also very useful in other domains, such as legged locomotion [6], where the possibility of storing energy on the elastic elements ([7], [8]) can be used in walking robots to alternatively transfer gravitational-potential and kinetic energy within each stride, minimizing the energy consumption.

Authors are with Centro Interdipartimentale di Ricerca "E. Piaggio", University of Pisa, 56126 Pisa, Italy {manuel.catalano,riccardo.schiavi,bicchi}@centropiaggio.unipi.it

As a further important motivation for VSAs, Haddadin et al. [9] showed how a mechanical elasticity between link and gearbox is instrumental to protect the robot mechanical structure, reducing peak forces during impacts against hard surfaces.



Fig. 1. VSA-HD, the new VSA prototype.

The effective implementation of VSAs is an outstanding research issue in robotics, where many different approaches are being pursued. One notable early example are pneumatic (McKibben) muscles [10], [2], although the need for a compressed air source represent a drawback for several applications. While new advanced materials, such as electroactive polymers, are being actively investigated [11], most current and near-future implementations use mechatronic solutions with different arrangements of electromechanical components, such as induction motors, gearboxes, and (non-linear) springs. For instance, the DLR VS-Joint ([12]) adopts a two motors - two gearboxes configuration: a motor is connected to the link through an Harmonic Drive (HD) gearbox and controls the equilibrium position of the link, while a (smaller) motor is connected to the nonlinear elastic element through a worm. Thanks to the non-backdrivability of the worm the VS-Joint maintains stiffness without exerting torque. The nonlinear elastic element is based on a set of spring acting on a cam profile, whereby the stiffness shape can be adapted to the task by designing the proper cam profile. As another example, the MACCEPA ([13]), originally designed for walking systems, consists of two geared motors and a non linear elastic element. Each motor chassis is rigidly connected to a link and the motor output shafts are interconnected by two lever arms and a linear spring. As in the preview design the two motors act independently on equilibrium position and stiffness of the

output shaft. Its evolution, the MACCEPA 2 ([14]) allows to design the stiffness-angle function by introducing a profiled disk, instead of the lever arm, acting on the linear spring. Rather than using one actuator for each degree of freedom (position and stiffness) in the agonistic-antagonistic (*A-A*) configuration both motors are employed to produce torque at the output shaft. Schiavi et al. in [15] propose the VSA-II, an *A-A* arrangement in which two geared motors are connected to the nonlinear elastic elements. Those elements are implemented by connecting a linear torsion spring to a couple of 4-bar linkages. Motors moving in opposite directions act on the stiffness, otherwise moving on the same direction they change the output shaft equilibrium position. Main difference with respect to the previous arrangements is that the *A-A* approach allows either motors to push and pull the link, enabling to transfer to output shaft all the generated torque. A basically similar component arrangement was proposed for the Variable Stiffness Joint (VSJ) by Choi et al. in [16]. In this arrangement, each motor is connected to the nonlinear elastic element by a gearbox. The variable stiffness is implemented by 4 leaf springs whose active length are controlled by pivots driven by 4-bar linkages. A difference between the motor positions causes a different equilibrium configuration for the 4-bar linkages, consequently changing the stiffness; otherwise motor motions leaving unchanged the relative position affects only the output shaft equilibrium position.

Although the various VS actuators have different characteristics (e.g. stiffness shape, maximum torque, component arrangement), most of them are composed by the same set of basic components: motors, gearboxes, and nonlinear elastic elements. The design of an element is generally related to the shape or the magnitude of a characteristics (e.g. angular displacement - stiffness, and stiffness range). On the other hand, the interconnection of components is mainly related to more general properties like *A-A* arrangement as in VSA-II, or explicit stiffness variation (*ESV*) as in VS-Joint. The possibility of changing the stiffness at the output joint, and more generally the high number of design parameters for VSAs, highlight the need for new criteria taking into account the new possibilities offered by these actuators. The criteria must enable a comparison between the different implementations of the general concept, and guide through the design process.

Section II introduces the matrix model, hypotheses and numerical filters used to enumerate the configuration layouts based on the selected basic components. The quasi-static model of the generic layout is proposed in Sec. III. In Sec. IV a preliminary set of tools to analyze VSA performance, and the inherited classification is carried out. Finally in Sec. V some preliminary characteristics of the VSA-HD, the prototypical implementation of a layout, is proposed.

## II. COMPONENTS AND CONNECTIONS

As discussed in the previous section a VSA is composed by basic elements, which we will distinguish in *components*,

including motors, gearboxes, link (output shaft) and mechanical frame, and mechanical *connections*, which we will classify as rigid, elastic, and free.

From a design specification point of view this article is focused on actuators capable of changing independently and simultaneously the stiffness and position at the output shaft. This requires at least two motors on the mechanical arrangement: for the sake of simplicity in the following only systems composed by two motors will be investigated. Electromechanical motors are often used in robotics equipped with gearboxes enabling high torque generation at low speed. To include these elements in the analysis, a specification of a gearbox model must be introduced. In the following, we will consider Harmonic Drive gearboxes because of their small axial footprint, the near-zero backlash, and the high ratio between reduction and weight or volume. HD systems are composed by tree elements: the *Wave Generator (WG)* an elliptical disk and an outer bearing; the *Flex Spline (FS)* a flexible element, internally connected by an elliptical bearing with *WG*, and externally teeth equipped; and the *Circular Spline (CS)*, a rigid ring with a different number of teeth on the inside. When the *WG* rotates the teeth on the major axis of *FS* get engaged with the corresponding on *CS*. For each revolution of the *WG* major axis of *FS* gets a displacement with respect to *CS* proportional on the difference of teeth, thus implementing the reduction ([17]). Fig. 2 illustrates the graphical representation of a layout (SX)

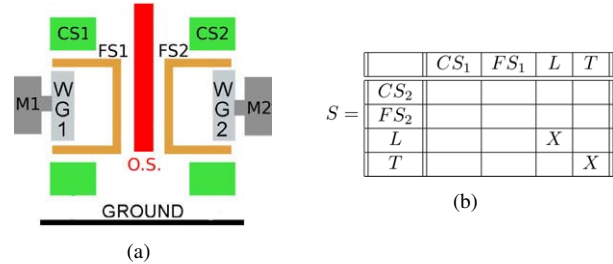


Fig. 2. Graphic (a) and matrix (b) representation of a layout without linkages. Motors and WGs (gray) are not considered in the analysis.

where no connections between basic elements are done.

To be able to study all the possible component arrangements some assumptions have to be done a priori to reduce the problem complexity and the magnitude of the solutions. It will be noticed that the pursued approach can be extended to more complicated or specific designs by adapting the set of rules explained in this section. For instance, to cope with planetary gearboxes we can consider as functionally equivalent the couples *CS*-annulus, *FS*-planet carrier, and *WG*-sun. On the other hand along the performance analysis kinematic differences have to be taken into account.

### A. Hypothesis

To enable a mathematical representation of the component interconnection and to include in the solution domain only actuators ensuring the stiffness controllability we have to assume some hypotheses.

1) *Symmetrical specs*: To reduce the solution space, without loss of generality, we can assume that the two motors and the two HDs have the same performance in terms of generated torque and reduction ratio. This hypothesis do not harms the abstraction since the effects of these parameters can be represented by a scaling factor in the layout performance.

2) *Reduction*: To enable the use of the HD as gearbox we need to connect the motor output to the *WG*. This hypothesis, needed to adopt smaller motors, is commonly assumed for robotic systems.

3) *Non-linear elasticity*: The stiffness at the VSA output shaft can be defined as  $\sigma = -\frac{\partial \tau}{\partial \theta} = -\frac{\partial f(\theta)}{\partial \theta}$ , where  $\tau$  is a disturbance force applied from the external,  $\theta$  the resulting displacement on the shaft, and  $f(\theta)$  is the force-displacement characteristic of the elastic element. To enable a stiffness variation  $f(\theta)$  have to be a non-linear function.

4) *Bidirectional elasticity*: Only bidirectional elastic elements will be taken into account.

5) *No limitation on link displacement*: Although robotics devices often include limits for the angular displacement at the joints, the actuators seldom have this limitation.

## B. Mathematical Representation

If we assume that no connection can be done inside to a HD, a matrix representation (Fig. 2) can be used to represent both all the configurations, where 0 and 1 mean no and elastic connection respectively,  $CS_i$ ,  $FS_i$  are the circular and flex spline of the HDs,  $L$  is the VSA output shaft, and  $T$  is the mechanical frame. Many of the following criteria are based on the sum of the elements on a row or column; consequently to enable the numeric representation of a rigid connection the value of 5 can be adopted. This value is guarantee to be greater than the sum of elements of any rows or columns composed by only elastic connections.

## C. Filters

By only applying the matrix representation the solutions are all the configurations composed by 6 basic elements ( $FS_1$ ,  $CS_1$ ,  $FS_2$ ,  $CS_2$ ,  $L$ , and  $T$ ) and 3 possible connections. Assuming that no  $L-L$  and  $T-T$  connections can be done, the solution space is represented by all the possible configurations of 14 connections ranging in 3 values ( $3^{14}$ ). Thanks to the matrix representation numerical filters can be used to isolate the configurations satisfying all the hypotheses.

1) *Symmetry*: Because of the Hyp. II-A.1 and II-A.4 symmetrical solutions result to be equivalent, thus allowing to eliminate a matrix if its symmetrical has been taken into account.

2) *No Link Limits*: To avoid element configurations causing limits on the output link displacement (Hyp. II-A.5) cannot be a straight or inherited connection between link and frame. Direct connections can be avoided by imposing

$$S_{ij} = 0 \quad \forall i, j \in \{3, 4\} .$$

To avoid inherited connection all the matrix containing a closed path between  $L$  and  $T$  have to be filtered.

3) *Gearbox 1*:  $L$  and  $T$  have to be connected at least to one element of both HDs to enable the torque transfer

$$\begin{aligned} L : S_{13} + S_{23} > 0 \quad \text{or} \quad S_{31} + S_{32} > 0 , \\ T : S_{14} + S_{24} > 0 \quad \text{and} \quad S_{41} + S_{42} > 0 . \end{aligned}$$

4) *Gearbox 2*: To preserve the reduction effect of the HDs all their components have to be connected at least to another on the assembly, this will be guaranteed if all the following conditions are satisfied

$$\begin{aligned} \sum_{i=1}^4 S_{1,i} \neq 0 \quad \sum_{i=1}^4 S_{2,i} \neq 0 \\ \sum_{i=1}^4 S_{i,1} \neq 0 \quad \sum_{i=1}^4 S_{i,2} \neq 0 . \end{aligned}$$

5) *Gearbox 3*: No rigid or elastic connection can be placed between the  $CS$  and the  $FS$  of one HD to avoid bounds on their relative positions. To filter inherited connections all the configurations including a closed path between the elements of an HD have to be filtered. For instance connections between the elements of one HD through the elements of the other can be avoided imposing

$$\begin{aligned} S_{i,1} \neq 0 \quad \text{or} \quad S_{i,2} \neq 0 \quad \forall i = 1, \dots, 4 \\ S_{1,i} \neq 0 \quad \text{or} \quad S_{2,i} \neq 0 \quad \forall i = 1, \dots, 4 . \end{aligned}$$

6) *Gearbox 4*: A rigid connection between  $CS$  and  $FS$  of the HDs harms to independently control the motors. This condition can be avoided by imposing

$$S_{11} + S_{22} < 10 \quad \text{and} \quad S_{12} + S_{21} < 10 .$$

7) *Decoupled Inertia*: The presence of rigid links between a HD and both  $L$  and  $T$  brings a rigid connection between at least one of the motors; thus arising to impose

$$\begin{aligned} S_{13} + S_{24} < 10 , \quad S_{14} + S_{23} < 10 \\ S_{31} + S_{42} < 10 , \quad S_{41} + S_{32} < 10 . \end{aligned}$$

Any closed path composed by rigid connections between these elements produce the same effect.

8) *Variable Stiffness 1*: To enable stiffness variation at the output shaft the system configuration must include at least two elastic connections. From a matrix representation perspective at least two matrix elements must be equal to 1

$$\exists i_1, i_2, j_1, j_2 : (i_1, j_1) \neq (i_2, j_2) , S_{i_1, j_1} = S_{i_2, j_2} = 1 .$$

## D. Layout

All the 140 layouts obtained after the filtering process differ from the mechanical point of view. Those layouts can be grouped from a functionality perspective in order to perform classification and/or performance analysis. On the other hand all of them can be taken into account during the design process, to cope with the mechanical differences (e.g. load capacity or mechanical complexity).

1) *Variable Stiffness 2*: Only elastic elements controlled by the motors produce a controllable stiffness contribution. Not controlled elements only affect the mechanical design, not the layout functional properties. Due on that layouts containing passive elastic connections can be grouped.

2) *Rigid Redundancy*: Configurations based on a path composed by 3 elements rigidly connected are functionally equivalent since the third connection is redundant.

### III. LAYOUT MODELING

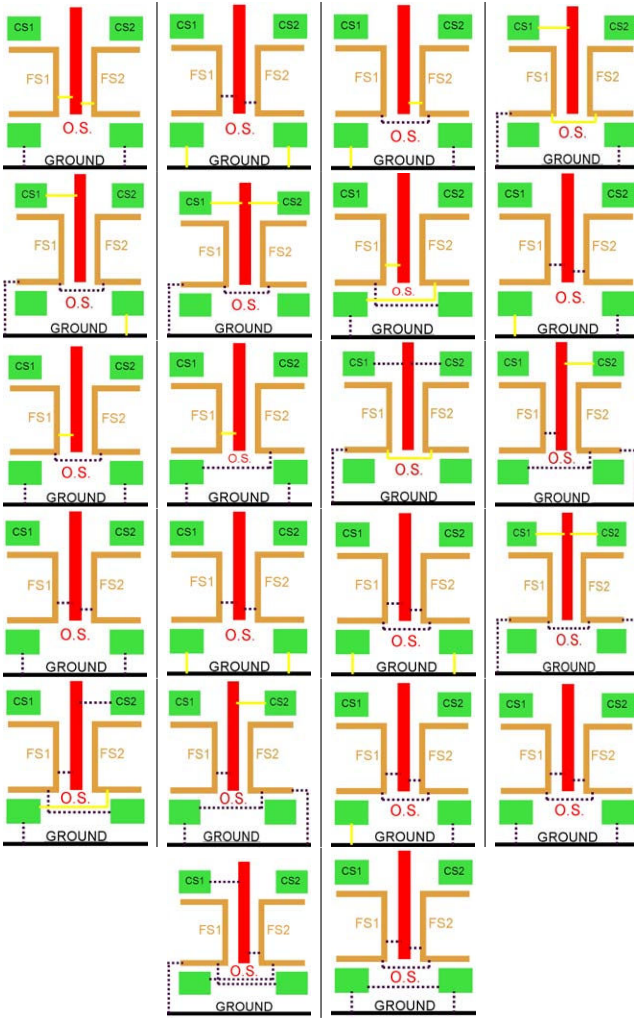


Fig. 3. Graphical representation of the 22 layouts. Yellow lines represents rigid connections, dashed black lines represents elastic connections.

3) *Elastic redundancy*: Layouts including an elastic and a rigid connection between the elements of one of the following terms

$$\begin{aligned} & (FS_i, L, FS_j), \quad (FS_i, L, CS_j), \quad (FS_i, T, FS_j), \\ & (FS_i, T, CS_j), \quad (CS_i, L, CS_j), \quad (CS_i, T, CS_j), \end{aligned}$$

$\forall i, j \in \{1, 2\}$  are functionally equivalents to systems where a third connection on the term exists, open or elastic.

4) *Reduction equivalency*: Because of Hyp. II-A.2 and II-A.4 layouts where the connection of an HD are exchanged can be considered equivalent, e.g. the systems

$$Sa = \begin{vmatrix} 0 & 0 & 0 & 1 \\ 0 & 0 & 5 & 0 \\ 0 & 5 & 0 & 0 \\ 1 & 0 & 0 & 0 \end{vmatrix} \quad Sb = \begin{vmatrix} 0 & 0 & 0 & 5 \\ 0 & 0 & 1 & 0 \\ 0 & 1 & 0 & 0 \\ 5 & 0 & 0 & 0 \end{vmatrix}$$

present a reduction ratio at the HDs differing only for the 2%. Such variation of the reduction ratio happens on HD when, fixed  $WG$  as input,  $FS$  is used as referring element and  $CS$  as output and can be neglected from the functionality perspective.

The filtering process highlights 22 layouts (Fig. 3) differing from the topological configuration. It should be noticed that these layouts include many of the actuators already presented by the community research; e.g. the second layout represents the VSA-II [15]. HDs are used as usual gearboxes and elastic bidirectional connections are resnet between them and the output joint shaft.

It is possible to introduce a mathematical model able to describe all of them by specifying a model of each component and connection, thus enabling a comparison between the layouts. The components inertia are more related to the mechanical implementation than to the mechanical layout; to avoid these effects a quasi-static model is adopted.

The motors can approximated by their electrical characteristic

$$\omega = \frac{V}{k_c} - C_0 \frac{R_a}{k_c^2} \tau, \quad (1)$$

where  $V$  is the supply voltage [V],  $\omega$  the angular velocity [rad/sec],  $\tau$  the output torque [Nm],  $R_a$  the armature resistance [ $\Omega$ ], and  $C_0$  an opportune conversion factor. The Harmonic Drive Model 2 proposed by Tuttle in [17] is adopted for the HDs. In this translational model HD elements are represented by planes, whose sloping is related to the reduction ratio. The evolution of the contact point between  $CS$  and  $FS$  is represented by translations along the  $y$ -axis, whereas movements along the  $x$ -axis represent system elements rotations. According to Hyp. II-A.1 and II-A.3 the nonlinear elasticity is modeled by the function  $K \sinh(\theta)$ , where  $\theta$  is the angular displacement between the interconnected elements, and  $K$  the elastic constant.

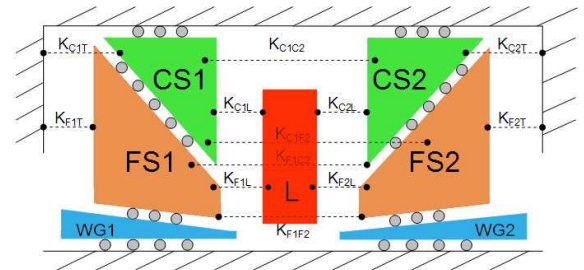


Fig. 4. Translational model of a generic layout including all the possible linkages.

Neglecting effects due on friction, plays, and rigidity of  $FS$ , the complete model can be expressed by the



## Differential-Algebraic Expression (DAE) system

$$\left\{ \begin{array}{l} x\dot{W}_1 = \frac{V_1}{k_c} - C_0 \frac{R_o}{k_c^2} F_{w1} \\ x\dot{W}_2 = \frac{V_2}{k_c} - C_0 \frac{R_o}{k_c^2} F_{w2} \\ 0 = K_{F_1 G} sh(x_{F_1}) + K_{F_1 C_2} sh(x_{F_1, C_2}) + \\ K_{F_1 F_2} sh(x_{F_1, F_2}) + K_{F_1 L} sh(x_{F_1, L}) + N F_{w1} \\ 0 = K_{F_2 G} sh(x_{F_2}) - K_{F_1 F_2} sh(x_{F_1, F_2}) - \\ K_{C_1 F_2} sh(x_{C_1, F_2}) + K_{F_2 L} sh(x_{F_2, L}) + N F_{w2} \\ 0 = -K_{C_1 G} sh(x_{C_1}) - K_{C_1 L} sh(x_{C_1, L}) - \\ K_{C_1 C_2} sh(x_{C_1, C_2}) - K_{C_1 F_2} sh(x_{C_1, F_2}) + \\ (N+1)F_{w1} \\ 0 = -K_{C_2 G} sh(x_{C_2}) + K_{C_2 L} sh(x_{C_2, L}) + \\ K_{C_1 C_2} sh(x_{C_1, C_2}) + K_{F_1 C_2} sh(x_{F_1, C_2}) + \\ (N+1)F_{w1} \\ 0 = K_{C_1 L} sh(x_{C_1, L}) + K_{C_2 L} sh(x_{C_2, L}) + \\ K_{F_1 L} sh(x_{F_1, L}) + K_{F_2 L} sh(x_{F_2, L}) + F_L, \end{array} \right.$$

where  $x_{ij} = x_i - x_j$  is the difference between the position of two elements,  $F_{w1}$ ,  $F_{w2}$  and  $F_L$  the motors and external load, and  $N$  the reduction ratio. To represent all the 3 possible connections we assume  $K_i \in \{0, 1, \infty\}$ . The complete scheme is reported in Fig. 4. The solution of the DAE system with respect to the inputs ( $V_1$ ,  $V_2$  and  $F_L$ ) is the temporal displacement evolution of the components ( $x_i(t)$ ).

The workspace of an elementary motor is fully described by the equilibria solutions of Eq. 1, or its graphical representation  $\langle \tau, \omega \rangle$ . This approach can be extended to VSAs taking into account the stiffness ( $\sigma$ ) as further degree of freedom. Fixed the admissible range for the actuators

$$|V_i| \leq V_M \quad i \in \{1, 2\}$$

where  $V_M$  is the maximum motor voltage, the DAE system admits equilibria solution if, and only if,  $F_L$  is lower than the maximum force that the motors can transfer to the link  $F_M$ , that can be evaluated given  $V_i$  (Eq. 1) and the layout configuration. Fig. 5 shows the solutions ( $\tau$ ,  $\omega$ ,  $\sigma$ , at the output shaft) obtained by solving the DAE for all the suitable values. The isometric view not only gives information about the working volume but also on the topology, more over the projections can be used to extract intrinsic properties of the layouts. For instance, the projection on the  $\langle \sigma, \tau \rangle$  gives information on the relation between the external load and the stiffness range, whereas the projection on  $\langle \tau, \omega \rangle$  replicates an usual motor chart.

## IV. CLASSIFICATION AND PERFORMANCE ANALYSIS

To simplify the layout comparison, the  $\langle \tau, \omega, \sigma \rangle$  charts can be normalized with respect to the maximum motor torque and velocity. The normalizer stiffness value is evaluated as the maximum stiffness produced by a geared motor compressing the nonlinear spring.

Either *ESV* and *A-A* macro-families can be identified by analyzing the charts. In *ESV* actuators one motor controls the stiffness, while the other is related to the equilibrium position of the output. Otherwise in *A-A* layouts both motors act on stiffness and link position at the same time. *ESV* actuators (Fig. 6e) have a quasi-prismatic working volume, meaning that an external load do not reduce the stiffness

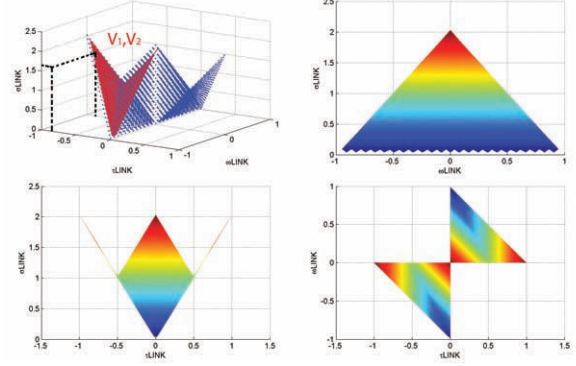


Fig. 5. Graphic representation of DAE system equilibria solution for a particular layout; 3D chart and relative projection. In red  $V_1$ ,  $V_2$  surface.

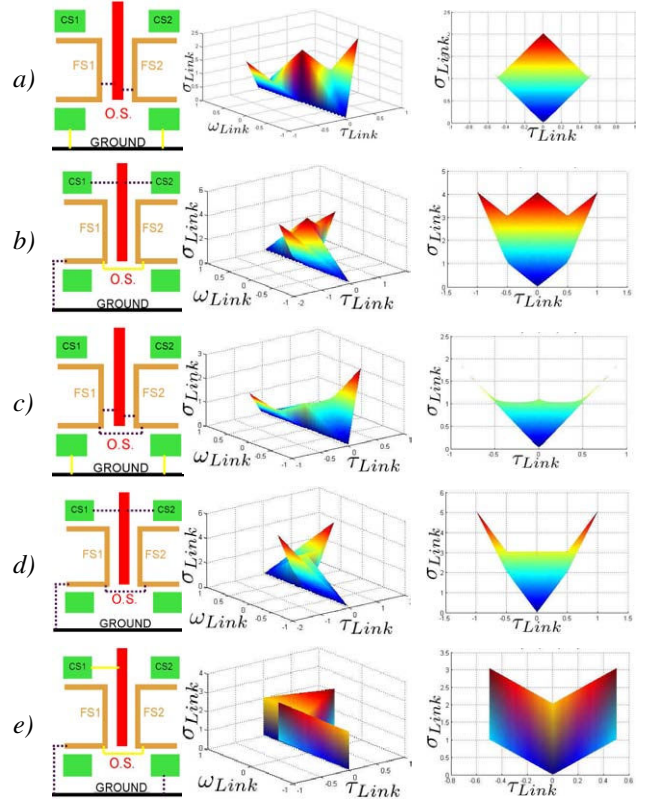


Fig. 6. Layout schema, Working Volume and projection on  $\langle \sigma, \tau \rangle$  plane of the 5 selected systems.

range. Otherwise *A-A* layouts have an irregular shape but the allowable torque at the output joint is double with respect to *ESVs*. *A-A* actuators can be more specified with respect to the presence of a cross-link between the elements of the HDs. From a mechanical perspective the cross-link prevents motors to set the maximum deformation at the elastic element. Unconnected actuators (Fig. 6a and 6b) join the maximum stiffness ( $\sigma_M$ ) for both  $\tau = 0$  and  $\tau = \tau_M$  (maximum torque), otherwise cross-linked actuator charts have only a maximum, as these actuators can reach  $\sigma_M$  only at  $\tau = \tau_M$  (Fig. 6c and 6d). A more specified taxonomy have to take into account the connection symmetry with respect to the

output shaft. The stiffness profile of systems characterized by symmetric linkages has thinner wings (Fig. 6a and 6c) than the asymmetric (Fig. 6b and 6d), this property is clearly showed by the  $\langle \tau, \sigma \rangle$  chart (Fig.5) and due on the unbalanced elastic connection.

As for off-the-shelf electromechanical motors, charts are not sufficient for a complete characterization. The possibility to vary the stiffness at the output joint shaft brings to define some new parameters

- 1) Working Volume ( $WV$ ): delimited by the external surface of the chart is related to the allowable working conditions of the system.
- 2) Real Working Volume Fitting ( $RWVF$ ):  $WV$  is not related to the shape of the working conditions. From

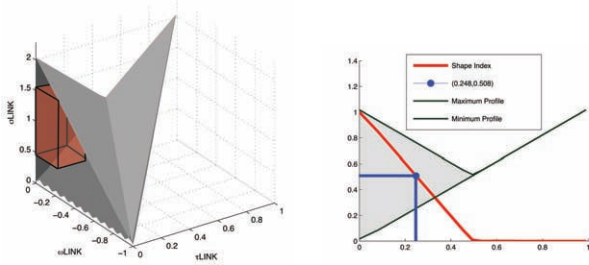


Fig. 7. Real Working Volume Fitting (SX) and Stiffness Breakdown (DX).

an application point of view usually the Needed Working Volume ( $NWV$ ) is defined as the volume  $|\langle \tau, \omega, \sigma \rangle| \in \langle \tau_M, \omega_M, \sigma_M \rangle$ ;  $RWVF$  index take into account the volume exceeding such prismatic volume and can be evaluated as

$$RTVF = \frac{NWV}{WV}.$$

- 3) Maximum Torque ( $\tau_M$ ): this parameter have to be considered mainly because of the differences between  $ESV$  and  $A-A$  layouts.
- 4) Maximum Stiffness ( $\sigma_M$ ): as previously explained  $\sigma_M$  is reached on different values of  $\tau$  depending on the layout.
- 5) Stiffness Velocity ( $\dot{\sigma}$ ): the time needed to change  $\sigma$  is one of the most important parameters on VSAs; an indicator can be defined as  $\dot{\sigma} = \frac{\Delta\sigma}{T_{ass}} \Big|_{\tau_M=0}$ , where  $T_{ass}$  is the time needed to join the maximum stiffness under maximum motors activation and negligible external disturbances ( $\tau = 0$ ).
- 6) Stiffness breakdown ( $S_b$ ): the stiffness range of  $A-A$  actuators depends on the external torque. We define  $S_b$  as the  $\tau$  value corresponding to the half of the maximum stiffness (Fig. 7).

Table I summarize the index values for the 5 layouts proposed in Fig. 6.

It can be noticed that  $S_b$  is not defined for  $ESV$  actuators, as they have small correlation between stiffness range and external torque. On the other hand the allowable torque at the output shaft of those systems is the half of  $A-A$  actuators. Analyzing  $A-A$  sub-families we can notice that asymmetric

	WV	$\tau_M$	$\sigma_M$	$\bar{\sigma}_M$	$\dot{\sigma}$	$S_b$
a	0.16	1	2.02	2.02	0.92	0.25
b	0.65	1	4.07	4.07	0.65	0.5
c	0.09	1	2.04	1.10	0.92	0.25
d	0.41	1	5.08	3.07	1.10	0.375
e	0.5	0.5	3.04	2.03	0.73	X

TABLE I  
INDEX VALUES OF THE LAYOUTS SHOWED IN FIG. 6.

systems have greater  $S_b$  and  $WV$ , on the other hand cross-linked ones presents lower  $\dot{\sigma}$ . A deep analysis of all the 22 layouts highlights that most of these parameters increase with the number of elastic connections and consequently with the mechanical complexity, whereas the connection schema is strictly related to the behaviour, e.g. the layouts Fig. ?? and Fig. ?? have the same kind and number of connections but a complete different behaviour.

## V. PHYSICAL IMPLEMENTATION

To verify the mechanical complexity of the layouts selected on the preview sections the Modular Variable Stiffness (VSM) prototype illustrated in Fig. 8 has been realized. The

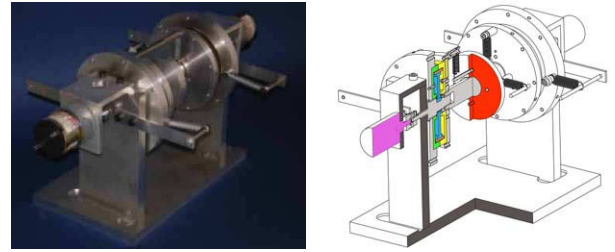


Fig. 8. Modular VSA used to test the different basic elements interconnections. In the schematic all the basic elements can be identified.

VSM is composed by a couple of DC motors and pancake HDs, and a modular connection system. The presence of a Dynamic Spline ( $DS$ ) is the main difference between these particular HDs and the traditional.  $DS$  is a circular rigid element having the same number of teeth than  $FS$ , thus ensuring the homokinetic motion between these two elements. All the active system components (motors and HD elements) are related by plain bearings and are free to rotate one respect to the other. The modular connection system allows to replicate all the connections of the layout matrix. Rigid beams are employed to implement rigid connections, whereas elastic connections are realized by linear traction springs and lever arms. With reference to Fig. 9, the non linear displacement of the spring ( $s$ ) is

$$s = \sqrt{(s_0 + r(1 - \cos(\delta(\theta)))^2 + (r \sin(\delta(\theta)))^2},$$

where  $s_0$  is the rest length of the spring,  $\theta$  the relative angle between the elements, and  $r$  the length of the lever arm.

Either chart/index analysis and implementation on VSM do not highlight a model as better for performance and complexity. For instance some layouts can have good performances but a very complex mechanical design because of

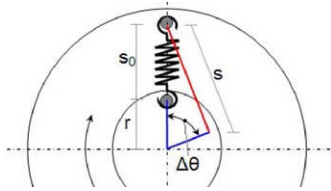


Fig. 9. Non linear elastic system of the Modular Variable Stiffness (VSM).

the number of connections or their positioning. Moreover, the application copes requirements, such as dimensions or reliability, on the mechanical design that have to be taken into account and are not considered by the proposed indexes.

Two layouts (Fig. 6b and 6e) have been selected as good balance between performances and mechanical complexity. Because of its mechanical simplicity the layout proposed in Fig. 6e has been implemented as first. Fig. 1 represents the prototype of the VSA-HD. The VSA-HD is an *ESV* actuator based on two rigid and two elastic connections. To reduce the overall weight and volume the design relies on the simpler connection schema of the layout family. The prototype adopts brushless motors (Maxon EC-PowerMax) and pancake HDs (100:1). Two pairs of 4-bar mechanisms, equipped with a linear spring ( $K=0.06$  [Nm/rad]), implement the nonlinear elastic elements adopting the configuration proposed in [15]. Table II reports some of the characteristics of the VSA-HD.

Rated Torque [Nm]	Repeated Peak Torque [Nm]	Momentary Peak Torque [Nm]	Velocity at rated torque [rpm]	Stiffness Range [Nm/rad]
6	10	14	37.6	0.3÷9

TABLE II  
VSA-HD PERFORMANCE PARAMETERS.

## VI. CONCLUSIONS AND FUTURE WORK

A mechanical enumeration of VSAs composed of two motors, two harmonic drive gearbox connected by rigid or nonlinear elastic elements is presented. From all the possible connection layouts a first selection is done by filtering all the systems not responding to functional properties such as the possibility to control the stiffness at the output joint shaft. A preliminary set of tools to compare the performance of VSAs is proposed and applied to group the layouts from a functionality perspective. Finally some preliminary characteristics of the VSA-HD, one of the two selected schema, has been presented.

Future work will involve both the experimental demonstration and validation of the proposed enumeration and the modeling and control of the VSA-HD, the selected prototype.

## VII. ACKNOWLEDGMENTS

Authors would like to acknowledge the useful work done by Andrea Gerace and Giorgio Grioli. This work was

partially supported by the VIATORS Specific Targeted Research Projects, funded under 7th Framework Programme of the European Community under Contract IST-231554, and by the PRIN 2007 project SICURA, funded by the Italian Ministry of Education, University, and Research (MIUR). The authors are solely responsible for its content.

## REFERENCES

- [1] A. Bicchi and G. Tonietti, "Dealing with the safety-performance trade-off in robot arms design and control," *IEEE Robotics and Automation Magazine*, vol. 11, no. 2, June, 2004.
- [2] R. Ham, T. Sugar, B. Vanderborght, K. Hollander, and D. Lefeber, "Compliant actuator designs," *Robotics & Automation Magazine, IEEE*, vol. 16, no. 3, pp. 81–94, September 2009.
- [3] B. Vanderborght, R. V. Ham, D. Lefeber, T. G. Sugar, and K. W. Hollander, "Comparison of mechanical design and energy consumption of adaptable, passive-compliant actuators," *The International Journal of Robotics Research*, vol. 1, no. 28, pp. 90 – 103, January 2009.
- [4] M. Uemura and S. Kawamura, "Safety evaluation of physical human-robot interaction via crash-testing," in *ICRA09*. Kobe, Japan: IEEE, May 12 – 17 2009.
- [5] S. A. Migliore, E. A. Brown, and S. P. DeWeerth, "Biologically inspired joint stiffness control," in *ICRA05*. Barcelona, Spain: IEEE, April 18 – 22 2005, pp. 4508 – 4513.
- [6] G. A. Pratt and M. Williamson, "Series elastics actuators," in *IROS*, 1995, pp. 399–406.
- [7] G. A. Cavagna, N. C. Heglund, and C. R. Taylor, "Mechanical work in terrestrial locomotion: two basic mechanisms for minimizing energy expenditure," *AJP - Regulatory, Integrative and Comparative Physiology*, vol. 233, no. 5, pp. 243 – 261, November 1977.
- [8] J. Yamaguchi, D. Nishino, and A. Takanishi, "Realization of dynamic biped walking varying joint stiffness using antagonistic driven joints," in *ICRA98*. Leuven, Belgium: IEEE, May 16 – 20 1998, pp. 2002 – 2029.
- [9] S. Haddadin, A. Albu-Schäffer, and G. Hirzinger, "Safety evaluation of physical human-robot interaction via crash-testing," in *Robotics: Science and Systems*, W. B. O. Brock; and C. Stachniss, Eds. The MIT Press, 2007.
- [10] D. Shin, I. Sardellitti, Y. Park, O. Khatib, and M. Cutkosky, *Design and Control of a Bio-inspired Human-Friendly Robot*, ser. Springer Tracts in Advanced Robotics. Springer Berlin / Heidelberg, March 28 2009, vol. 54, pp. 43–52.
- [11] F. Carpi, C. Menon, and D. D. Rossi, "An electroactive elastomeric actuator for all-polymer linear peristaltic pumps," *Mechatronics, IEEE/ASME Transactions on*, 2009.
- [12] S. Wolf and G. Hirzinger, "A new variable stiffness design: Matching requirements of the next robot generation," in *ICRA08*. Pasadena, CA, USA: IEEE, May 19 – 23 2008, pp. 1741 – 1746.
- [13] R. V. Ham, B. Vanderborght, M. V. Damme, B. Verrelst, and D. Lefeber, "MACCEPA, the mechanically adjustable compliance and controllable equilibrium position actuator: Design and implementation in a biped robot," *Robotics and Autonomous Systems*, vol. 55, no. 10, pp. 761–768, 2007.
- [14] B. Vanderborght, N. Tsagarakis, C. S. R. V. Ham, and D. Caldwell, "MACCEPA 2.0: Adjustable compliant actuator with stiffening characteristic for energy efficient hopping," in *ICRA09*. Kobe, Japan: IEEE, May 12 – 17 2009, pp. 544 – 549.
- [15] R. Schiavi, G. Grioli, S. Sen, and A. Bicchi, "VSA-II: A novel prototype of variable stiffness actuator for safe and performing robots interacting with humans," in *ICRA08*. Pasadena, CA, USA: IEEE, May 19 – 23 2008, pp. 2171 – 2176.
- [16] J. Choi, S. Hong, W. Lee, and S. Kang, "A variable stiffness joint using leaf springs for robot manipulators," in *ICRA09*. Kobe, Japan: IEEE, May 12 – 17 2009, pp. 4363–4368.
- [17] T. D. Tuttle and D. Timothy, "Understanding and modeling the behavior of a harmonic drive gear transmission," Cambridge, MA, USA, Tech. Rep., 1992.
- [18] *ICRA 2009, Proceedings of the 2009 IEEE International Conference on Robotics and Automation*. Kobe, Japan: IEEE, May 12 – 17 2009.
- [19] *ICRA 2008, Proceedings of the 2008 IEEE International Conference on Robotics and Automation*. Pasadena, CA, USA: IEEE, May 19 – 23 2008.